Analogs of the Golgi complex in microsporidia: structure and avesicular mechanisms of function

Galina V. Beznoussenko[1,*], Viacheslav V. Dolgikh[2,*], Elena V. Seliverstova[3], Petr B. Semenov[2], Yuri S. Tokarev[2], Alvar Trucco[1], Massimo Micaroni[1], Daniele Di Giandomenico[1], Peter Auinger[4], Igor V. Senderskiy[2], Sergei O. Skarlato[5], Ekaterina S. Snigirevskaya[5], Yan Yu. Komissarchik[5], Margit Pavelka[4], Maria A. De Matteis[1], Alberto Luini[1], Yuliya Ya. Sokolova[5,‡] and Alexander A. Mironov[1,‡,§]

[1]Department of Cell Biology and Oncology, Consorzio Mario Negri Sud, Via Nazionale, 66030 Santa Maria Imbaro (Chieti), Italy
[2]Laboratory of Microbiological Control, All-Russian Institute for Plant Protection, Russian Academy of Agricultural Sciences, Shosse Podbelskogo, 3, 189620, St. Petersburg–Pushkin, Russia
[3]Laboratory of Renal Physiology, Sechenov Institute of Evolutionary Physiology and Biochemistry, 44 Moris Torez Prospekt, St. Petersburg, Russia
[4]Institute of Histology and Embryology, University of Vienna, Schwarzspanierstrafle 17, A-1090 Vienna, Austria
[5]Institute of Cytology, Russian Academy of Sciences, Tikhoretsky Av., 4, 194064, St. Petersburg, Russia

*These authors contributed equally to this work
‡Principal investigators
§Author for correspondence (e-mail: mironov@negrisud.it)

Accepted 10 January 2007
Journal of Cell Science 120, 1288-1298 Published by The Company of Biologists 2007
doi:10.1242/jcs.03402

Summary

Microsporidia are obligatory intracellular parasites, most species of which live in the host cell cytosol. They synthesize and then transport secretory proteins from the endoplasmic reticulum to the plasma membrane for formation of the spore wall and the polar tube for cell invasion. However, microsporidia do not have a typical Golgi complex. Here, using quick-freezing cryosubstitution and chemical fixation, we demonstrate that the Golgi analogs of the microsporidia *Paranosema (Antonospora) grylli* and *Paranosema locustae* appear as 300-nm networks of thin (25- to 40-nm diameter), branching or varicose tubules that display histochemical features of a Golgi, but that do not have vesicles. Vesicles are not formed even if membrane fusion is inhibited. These tubular networks are connected to the endoplasmic reticulum, the plasma membrane and the forming polar tube, and are positive for Sec13, γCOP and analogs of giantin and GM130. The spore-wall and polar-tube proteins are transported from the endoplasmic reticulum to the target membranes through these tubular networks, within which they undergo concentration and glycosylation. We suggest that the intracellular transport of secreted proteins in microsporidia occurs by a progression mechanism that does not involve the participation of vesicles generated by coat proteins I and II.

Supplementary material available online at
http://jcs.biologists.org/cgi/content/full/120/7/1288/DC1

Key words: Golgi, Intracellular transport, COP-I vesicles, Microsporidia

Introduction

All cells secrete a diverse range of macromolecules that are used to modify their environment and to protect themselves. There is also a need to replace membrane proteins and lipids that are constantly degraded within the various compartments of the secretory and endocytic pathways. Therefore, eukaryotic cells synthesize proteins and lipids both for export and for delivery to specific compartments and the plasma membrane. Secreted and membrane proteins are synthesized on ribosomes that are attached to the cytosol surface of the endoplasmic reticulum (ER), whereas lipids are synthesized in the smooth ER. During their synthesis, proteins are transferred into the ER lumen or incorporated into the ER membrane and after folding they are transported along the secretory pathway. As they pass through the Golgi complex, both proteins and lipids undergo post-translational modifications (mainly glycosylation by Golgi glycosidases and transferases) and sorting. The basic mechanisms of intra-Golgi transport remain uncertain. Two mechanisms are particularly popular at present: the vesicular model and the cisterna maturation model (Beznoussenko and Mironov, 2002; Mironov et al., 2005). Both of these are based on the assumption that coat protein I (COP-I)-dependent vesicles participate in the transport of either cargo or Golgi enzymes.

The essence of the current version of the cisterna maturation scheme (Bonfanti et al., 1998) is that cargo progresses through the Golgi while remaining within the Golgi cisterna to which it was originally delivered, while the Golgi enzymes recycle back via COP-I-dependent vesicles. This model would require the Golgi enzymes to be enriched in these vesicles. However, our own recent study (Kweon et al., 2004) based on several complementary approaches showed that Golgi enzymes are depleted in actual COP-I-dependent vesicles. Furthermore, there are no COP-I-coated buds detectable on the last *trans*-cisternae (Ladinsky et al., 1999; Ladinsky et al., 2002) although some Golgi enzymes, such as sialyltransferase and fucosyltransferase, are present therein (Rabouille et al., 1995; Opat et al., 2001). These observations are at odds with the predictions of this model.

A further difficulty for the cisterna maturation model arises

from the kinetics of cargo exit from the Golgi that, according to this version, should be close to linear with respect to time. However, Hirschberg et al. (Hirschberg et al., 1998) have demonstrated that this kinetics is exponential [at least for the temperature-sensitive variant of the G protein of vesicular stomatitis virus tagged with a fluorescent protein (VSVG-FP)], suggesting that VSVG moves via a diffusion-based mechanism through continuities between heterogeneous compartments, rather than by cisterna maturation.

One way to potentially resolve these contradictions is to use minimal cellular systems. One promising candidate is microsporidia, the smallest intracellular eukaryotic parasite from the point of view of their physical (2-3 μm in diameter, depending on species) and genome (~2-3 Mb, on average) sizes (supplementary material Fig. S1). This cellular model demonstrates a range of the important advantages: (1) During sporogony, these cells appear to intensively synthesize spore-wall and polar-tube proteins in the ER and transport them to the forming structures. The N-terminal regions of the microsporidia spore-wall and polar-tube proteins contain signal peptides for ER translocation (Delbac et al., 1998; Keohane and Weiss, 1999; Bohne et al., 2000; Hayman et al., 2001). (2) According to data from the genome project of the human microsporidia *E. cuniculi* (Katinka et al., 2001), as with all other eukaryotes, these cells possess all of the most important and well-characterized protein machineries that are involved in co-translational translocation of polypeptide chains into the ER lumen, as well as in their intracellular transport, although some of these lack non-essential components. Similar regularities have been seen in *P. locustae* (http://jbpc.mbl.edu/Nosema/index.html). The presence of these (sometimes reduced) protein machines indicates that in microsporidia the process of protein secretion should be similar to that in mammalian cells. (3) In microsporidia, instead of the classical Golgi structure, only unusual membrane aggregates have been described, which have been described as 'vesicular' Golgi zones. At their late stages in intracellular development (when polar-tube formation begins) their Golgi becomes more prominent (Vavra and Larsson, 1999). (4) The stages in microsporidia development are easily distinguishable morphologically and thus these well-established and recognizable stages can allow the characterization of the microsporidia Golgi. The initial stage of microsporidia development, the meront, is characterized by the absence of any protein envelope outside the plasma membrane and very few membranous elements are present within its cytoplasm. The sporont is defined by the formation of a spore wall outside the plasma membrane, without the presence of a large Golgi and without forming a polar tube. The main features of the sporoblast are the formation of the polar tube and a large Golgi, and the oval shape of the cells. The electron-transparent growing envelope of the endospore defines a spore (Vavra and Larsson, 1999).

The disadvantage of this system is that microsporidia cells cannot be transfected with proteins or infected with viruses, and thus synchronization of intracellular transport in microsporidia has not been possible to date. Therefore, dynamic experiments are limited to an examination of protein localization during developmental stages. However, these stages of microsporidia development approximate the steps of intracellular transport.

The aim of the present study is to demonstrate the intracellular transport of secreted proteins in microsporidia cells and to determine whether this involves COP-I and COP-II vesicles. We have examined the stages of intracellular development of the microsporidia *P. grylli* and *P. locustae* to find and to characterize parasite structures that are equivalent to the Golgi of other eukaryotic cells. We demonstrate that the *P. grylli* and *P. locustae* Golgi analogs appear as networks of thin (25-nm diameter) branched tubules with cytochemical features of a Golgi, but without vesicles. These are positive for endogenous Sec13, as well as for exogenous γCOP and analogs of GM130 and giantin. Spore wall and polar tube proteins are transported from the ER to the plasma membrane and to the forming polar filament through these tubular networks (TNs), within which they are seen to be concentrated and glycosylated. Our data suggest that in microsporidia, ER-to-plasma membrane transport occurs by a progression mechanism that is independent of COP-I and COP-II vesicles.

Results

We used two microsporidia species: *P. grylli* (owing to the convenience of manipulations) and *P. locustae* (to make use of the database from the *Nosema locustae* Genome Project, http://jbpc.mbl.edu/Nosema/index.html), two very closely related species with genes that show about 95% identity (our unpublished observations) (see also Sokolova et al., 2005). Most of data presented here are from *P. grylli*; however, all of our conclusions were also confirmed in *P. locustae* (see supplementary material Figs S2-S4).

Golgi analogs in *P. grylli* at different stages in the life cycle

In early meronts (Fig. 1A), 300-700-nm clusters of 30-50 nm elongated and rounded profiles were visible, which were often connected to each other by thin (25-35 nm) tubules (Fig. 1B,C). In each meront, there were at least 5-7 such clusters, which were connected with the ER (Fig. 1B,C) and sometimes associated (connected) with the plasma membrane near clusters of protrusions (Fig. 1D,E).

To examine the three-dimensional (3D) structures of these clusters, we performed electron microscopy (EM) tomography reconstructions, with subsequent surface rendering. This revealed that these aggregates of round profiles were networks of branching and/or anastomosing, 25-40 nm diameter tubules that were connected with the nuclear membrane and the cisternae of the ER (Fig. 2A). Each tubular network (TN) consisted of two parts. One appeared as a network composed of 30-45 nm branching tubules, with some flattened domains at the level of the branches. Smooth tubules did not contain the visible dense coat that is similar to that of COP-I-coated buds or vesicles (Orci et al., 1986) or COP-II-coated buds (Bannykh et al., 1996). The second TN component was a less-branched network that was composed of varicose tubules, where the thinnest tubules had diameters of 25 nm. Isolated vesicles were not seen within the TNs, as revealed by three perpendicular views of the same single voxel of a number of round profiles that showed connections of vesicle-like structures with different structures in different virtual sections (Fig. 3A-D). To date, all of the ten tubular clusters that have been examined in each of the meronts, sporonts and sporoblasts after chemical fixation were connected to the ER cisternae and did not contain

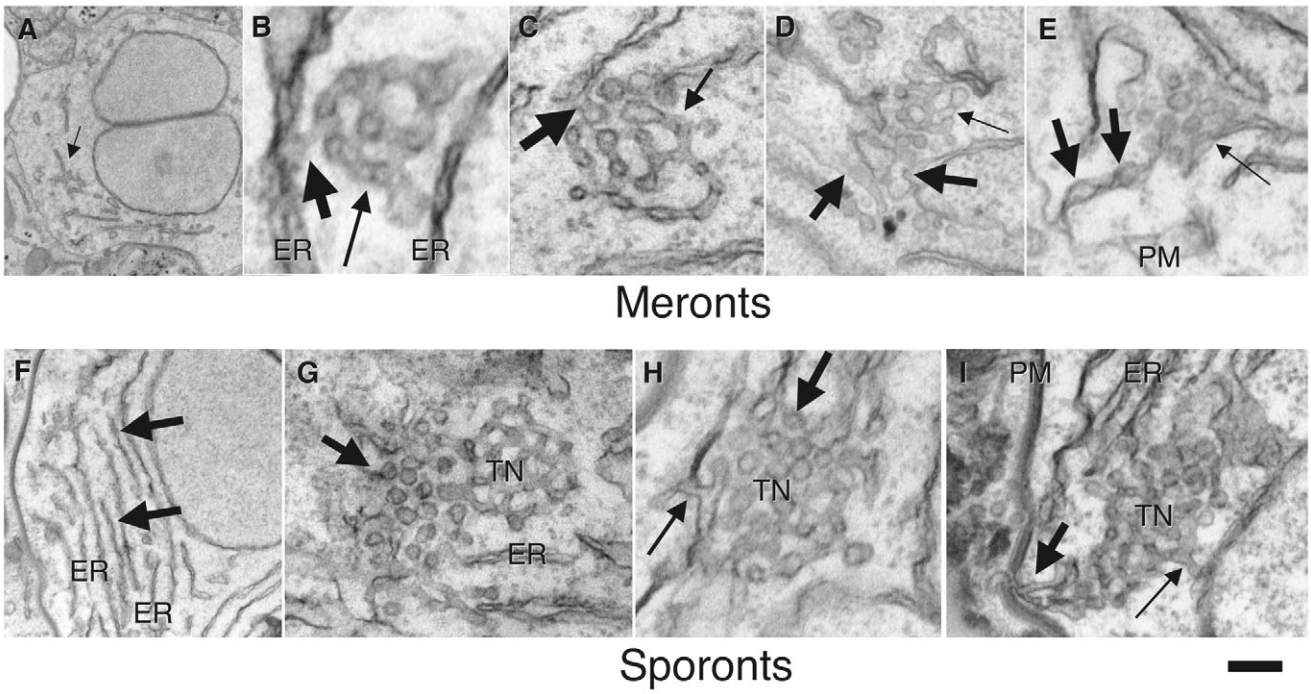

Fig. 1. Ultrastructure of the Golgi in microsporidia *P. grylli.* Cells from cricket fat bodies were infected with *P. grylli*, fixed and prepared for routine EM. (A-E) Clusters (300-700 nm in diameter, thin arrows) of elongated round profiles (TNs) in meronts, which are often connected with the ER (B,C, thick arrows) and sometimes to the plasma membrane (D,E, thick arrows). (F-I) In sporonts, the number of ER cisternae (F, thick arrows) and the size of the TNs (G-I, TN) are increased. TNs are mostly composed of round profiles (G,H, thick arrows) and often connected with the ER (H,I, thin arrows) and with the plasma membrane (I, thick arrow). Bar, 1400 nm (A); 130 nm (B); 160 nm (C); 270 nm (D,G,I); 1000 nm (F); 200 nm (E,H).

vesicles. About 90% of the TNs on serial sections exhibited connectivity with the ER, whereas only 10% showed connectivity with the plasma membrane. No TN was found with clear connections with both the ER and the plasma membrane. Thus, the early stages of microsporidia contain TNs that are connected to the ER and associated with the plasma membrane and that do not contain free vesicles.

In sporonts, the number of ER cisternae (Fig. 1F) and the size of the TNs increased two- to threefold (Fig. 1G-I). Some reached a diameter of 800-900 nm (Fig. 1I). Their 'vesicular' parts became more evident, and they appeared as aggregates of round profiles, most of which showed increases in diameter of up to 70 nm (Fig. 1G,H). Some tubules appeared to be more clearly connected with the plasma membrane (Fig. 1I). EM tomography reconstructions revealed that the tubules of the TNs contain almost double the number of varicosities than in earlier stages of microsporidia (Fig. 2E,F). However, again, no free vesicles were seen. The TNs became larger and were concentrated at one pole of the cell, forming a single large cluster. Surface rendering after EM tomography (Fig. 2E) demonstrated that the tubules of the TNs became less uniform in diameter, with varicosities at the branching points, but without vesicles and buds. In these sporoblasts, the tightly packed, cisterna-like membranes of the *trans*-Golgi remnants appeared near to the single large TN that was connected to the polar tube (our unpublished observations).

In most of these experiments, standard fixation techniques were used for EM. Although validated in numerous experiments, chemical fixation is always a potential source of artifacts. For instance, in theory, 50-60 nm vesicles exist in microsporidia, but they might be made to fuse with neighboring cisternae by the fixatives. This would mask the evidence for their existence. To overcome this problem, we used ultra-fast cryofixation, a virtually artifact-free method (McIntosh, 2001). The cells were fixed by high-pressure freezing (McIntosh, 2001) and then serially sectioned or subjected to electron tomography to establish the 3D structure of the TNs. Out of six TNs analyzed after freezing cryosubstitution, none were found to have isolated 50-60 nm vesicles (Fig. 2B, Fig. 3E).

Another potential reason for failing to observe the standard 50-60 nm, coatomer-dependent Golgi vesicles that are seen in other cell types is that these structures might be too transient to be seen with our experimental set-up. Given the significant number of TNs sectioned to date in this study, this would be very unlikely. However, despite this, we reasoned that if coatomer-dependent vesicles normally form but fuse immediately with the acceptor compartment, they should accumulate, and hence become detectable, if fusion is inhibited. The protein NSF is essential in the known pathways of Golgi membrane fusion (including fusion of COP-I vesicles to Golgi membranes) and it is present in the microsporidia genome (Katinka et al., 2001); the highly membrane-permeable reagent N-ethylmaleimide (NEM) under controlled conditions (Mironov et al., 2001; Kweon et al., 2004) can relatively selectively inactivate NSF. Fresh homogenates of fat bodies of infected *Gryllus bimaculatus* crickets were thus treated with NEM for 15 minutes on ice, and they were fixed

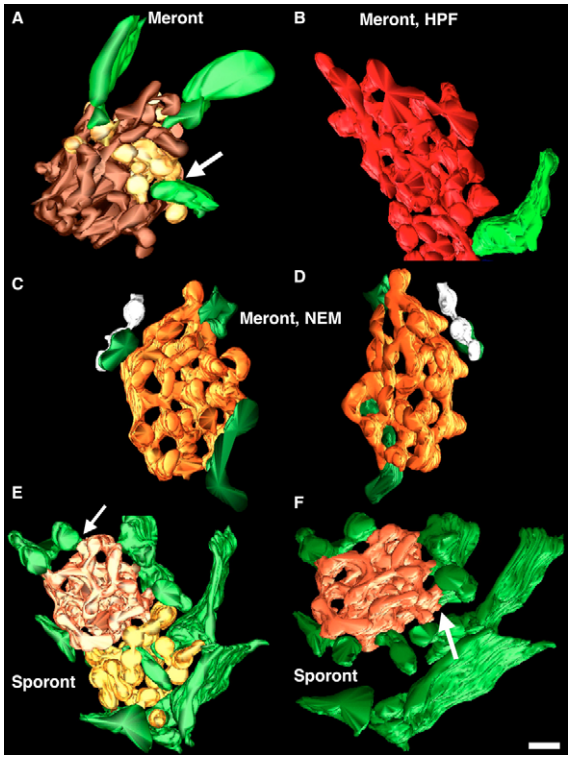

Fig. 2. Three-dimensional reconstructions of tubular networks in *P. grylli*. Cells from cricket fat bodies were infected with *P. grylli* and fixed chemically (A,C-F) or prepared by high pressure freezing and cryosubstitution (B). 200-nm-thick sections of microsporidia were subjected to EM tomography. (A) General overview of the meront TN surrounded by the ER (green), which contains tubular (brown) and varicose (yellow) parts. Arrow indicates connection between TN and ER. (B-D) TNs in meronts pretreated without (B) and with (C,D) NEM for 15 minutes. (E,F) In the sporont, the varicose part is larger, with the smooth tubular part still connected (E,F, arrows) to the ER (green). (B-D) TNs, red (B) or orange (C,D); ER, green. Bar, 80 nm (A-D); 100 nm (E,F).

15 minutes after wash-out of the NEM, with dithiothreitol (DTT). To verify the efficacy of this treatment, we counted the number of round profiles in the host cells after exposure to NEM [since NEM does not block vesicle formation, vesicles should accumulate in cells treated with this agent, as shown by Mironov et al. (Mironov et al., 2001)]. As expected, in the host cells, the round profiles with the appearance expected for COP-I vesicles increased in number to levels fivefold higher than basal values, confirming that NEM had inhibited vesicle fusion (Fig. 3G). However, when the microsporidia cells were examined, no accumulation of round profiles near and within the TNs was seen, further indicating that 50-60 nm vesicles never dissociate, even transiently, from the TNs (Fig. 2C,D, Fig. 3F,G).

In another approach, aluminium fluoride (AlF_4) was used to block the uncoating of COP-I vesicles (Cole et al., 1996), if they exist. Fresh homogenates of fat bodies of infected *G. bimaculatus* crickets were treated with AlF_4 for 20 minutes at 37°C, and then examined under EM. To verify the efficacy of this treatment, we also counted the number of round profiles in host cells after exposure to AlF_4. As expected, in the host cells, round profiles with the appearance expected for COP-I vesicles increased in number to levels threefold higher than basal values, whereas the Golgi stacks were consumed, confirming that AlF_4 had inhibited vesicle fusion (Fig. 3H). By contrast, when microsporidia cells were examined, no accumulation of round profiles near and within the TNs was seen, further indicating that 50-60 nm vesicles never dissociate, even transiently, from the TNs (Fig. 3I,J).

In summary, TNs are present at all stages of intracellular development of microsporidia (in meronts, sporonts and sporoblasts). These become more prominent as development progresses towards the formation of spores. The TNs do not contain buds and vesicles, and they are associated with or connected to the ER and the plasma membrane or the forming polar tube.

The tubular networks contain Golgi markers

To determine whether the TNs represent the Golgi, we used a well-known cytochemical reaction: prolonged treatment with 1% OsO_4 (without a preliminary fixation with aldehyde) (Novikoff and Goldfischer, 1961). In most eukaryotes, the glyco-residues (with a specific aldehyde-group content) located inside the lumen of the *cis*-Golgi (but not in any other intracellular compartments) convert OsO_4 into its insoluble oxides. Fig. 4A shows that prolonged treatment of meronts with an aqueous solution of 1% OsO_4 resulted in the precipitation of osmium black over the TNs, which was suggestive of them having a Golgi nature. Of interest, the osmium staining was higher in round profiles (Fig. 4A). To confirm the Golgi nature of the TNs, we determined whether thiamine pyrophosphatase, a marker of the *trans*-cisternae (Griffiths et al., 1989), was present in these microsporidia Golgi remnants. As expected (Vavra and Larsson, 1999), staining of the TNs was seen only in the late sporont (data not shown) (see also Sokolova et al., 2003). Additionally, we decorated the cryosections of infected cricket fat bodies with mannose-specific GNA-lectin conjugated with colloidal gold particles. GNA labeling was not seen in the microsporidia ER, but was visible over the polar tube, spore wall and TNs, suggesting that the process of glycosylation begins there (Fig. 4B).

Initially, a pAb generated against endogenous Sec13 from *N. locustae* (see supplementary material Fig. S5A) (V.V.D., unpublished results) labeled TNs mostly in meronts (Fig. 4E, and supplementary material Fig. S5F) and less in sporonts (Fig. 4F, and supplementary material Fig. S5G-I). Most of the labeling was present over elongated profiles, with much less over round ones.

To further test whether the TNs are of Golgi origin, we used a well-known approach based on the application of Abs derived from another species, with subsequent further characterization. We western blotted microsporidia extracts, using all of the known Abs against the COP-I components. To this end, the pAb raised against a full-length recombinant Sec21 (γCOP) from *Arabidopsis thaliana* (Pimpl et al., 2000) (note that γCOP from *P. locustae* has the maximal similarity with γCOP from *Arabidopsis*) recognized in both *P. grylli* and *P. locustae* a polypeptide of about 80 kDa (supplementary material Fig. S5B), the expected molecular mass for γCOP in *P. locustae* (http://jbpc.mbl.edu/Nosema/index.html, *Nosema locustae* Genome Project, Marine Biological Laboratory at Woods

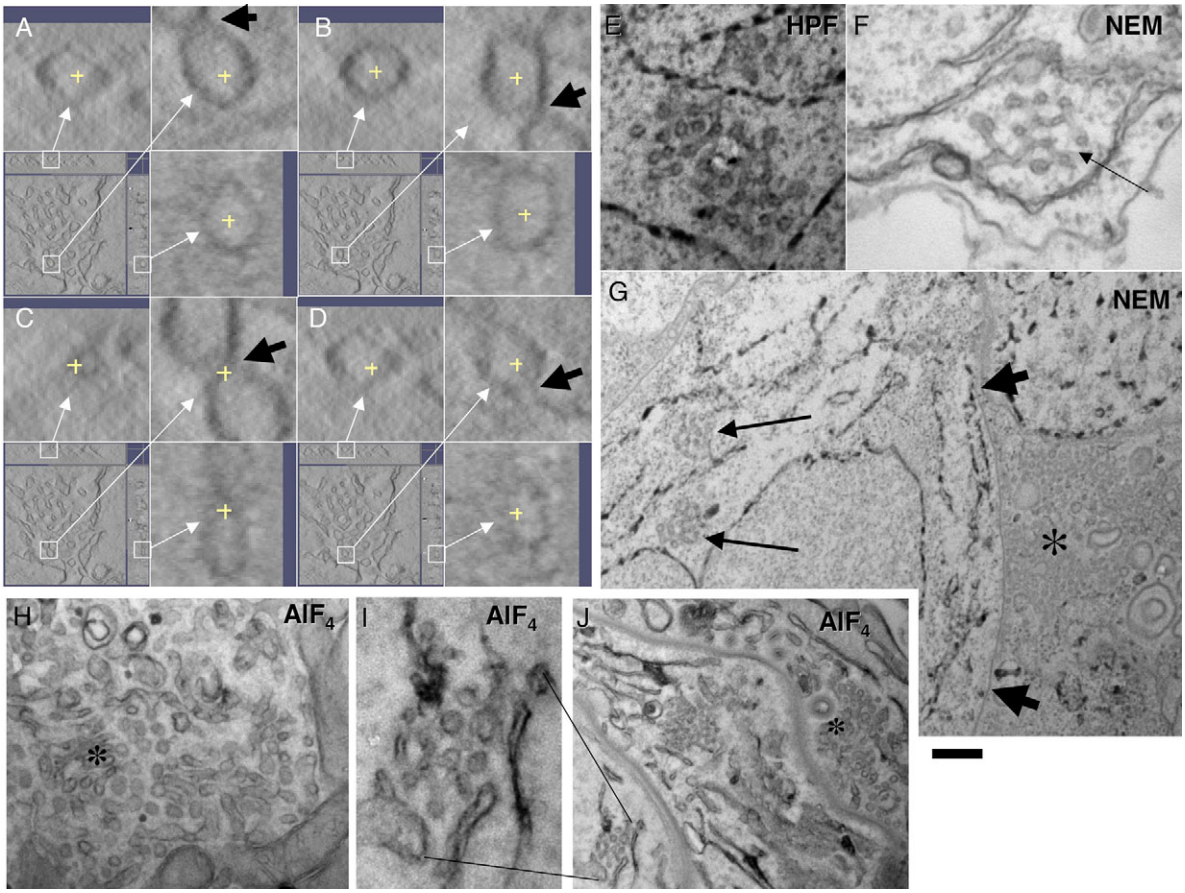

Fig. 3. The round profiles within the tubular networks are not vesicles, but varicose tubules. Cells from cricket fat bodies were infected with *P. grylli* and fixed and prepared for EM tomography (A-D), routine EM (F-J) or for EM by high pressure freezing and cryosubstitution (E). (A-D) 200-nm-thick sections of a meront as extracted virtual sections of part of a TN (with three perpendicular views of the same single voxel indicated by yellow crosses). Enlargements of the white boxes are indicated by white arrows. Thick arrows indicate connections between round profiles and other structures. (E-J) Samples were pretreated without (E) and with NEM for 15 minutes (F,G) or AlF_4 for 20 minutes (H-J). Thin arrows in F,G indicate TNs, thick arrows in G indicate microsporidia plasmalemma. Asterisks in G,H,J indicate the vesiculated Golgi of the host cell. Normal TNs are seen in microsporidia treated with both NEM (F,G) and AlF_4 (I,J). Bar, 120 nm (A-D, original sections); 35 nm (A-D, enlargements); 150 nm (E,F,H,I); 500 nm (G,J).

Hole), the closest relative of *P. grylli*. This pAb gave a highly specific labeling over the host vesicular-tubular clusters (VTCs) and Golgi (supplementary material Fig. S5C,D), and over the TNs in meronts, especially when its concentration was elevated in the presence of the most efficient agent for blocking background labeling, such as BSA-c (Fig. 4C). Most of the labeling was seen over round profiles and much less over elongated ones. This labeling increased in sporoblasts and sporonts near to the forming polar tubes (Fig. 4D), suggesting that a γCOP homolog was present in the TNs.

In addition, we revealed specific interactions of microsporidia proteins with pAbs against mammalian Golgi-matrix components: giantin and GM130. The anti-giantin Ab recognized a single band of 190 kDa in a membrane fraction from the *P. grylli* intracellular stages, but not from spores (see supplementary material Fig. S6A), while the anti-GM130 Ab interacted with an ~90-kDa band in both the microsporidia spores and the intracellular stages (see supplementary material Fig. S6B). The immunofluorescent labeling in meronts exhibited a spotty pattern, with the number of spots equal to the number and size of the TNs at this growth stage (see supplementary material Fig. S6C-E). Cryosectioning and immunogold EM demonstrated that both Abs specifically recognized the TNs described above at the early (Fig. 4G,H, see also Fig. 6C) and late (supplementary material Fig. S6F,G) stages of microsporidia development.

Thus, altogether these data demonstrate that the TNs possess cytochemical and immunochemical features of the *cis*-Golgi compartment, and the consequence of exchange of COP-II into COP-I on TNs is similar with that in ER-to-Golgi carriers in mammalian cells (Scales et al., 1997).

In microsporidia, the spore wall and polar tube proteins undergo glycosylation

If the TNs represent the Golgi in microsporidia, which is a minimal eukaryotic cell, they should participate in the intracellular transport of secretory proteins in some way. The most plausible candidates to demonstrate ER-to-plasma membrane transport in microsporidia cells are proteins exported out of the cell in the formation of the spore wall. In

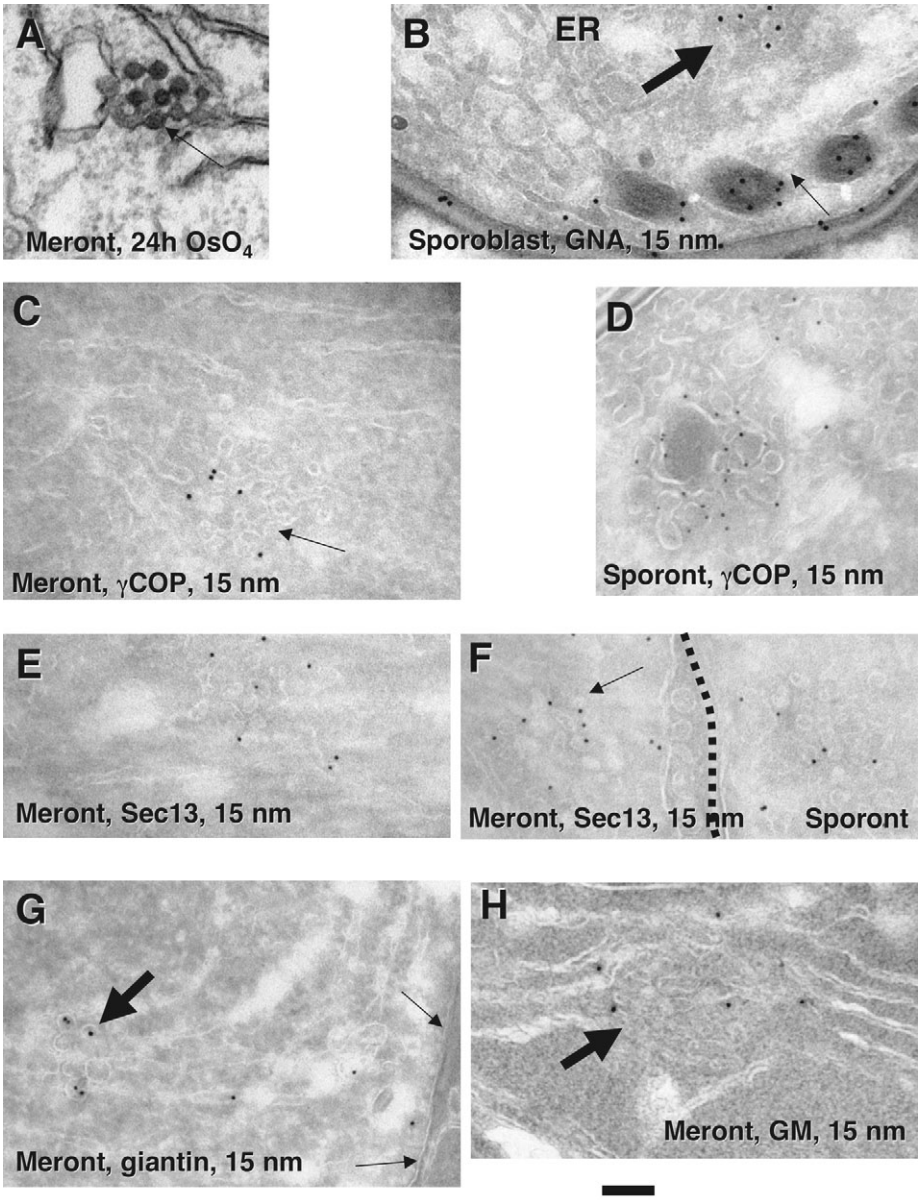

Fig. 4. Localization of *cis*-Golgi markers in the tubular networks. Cells from cricket fat bodies were infected with *P. grylli* and treated with an aqueous 1% solution of OsO_4 for 24 hours (A) or prepared for cryo-immuno EM (B-H). (A) Arrow shows TN stained with osmium black. (B) Immuno-gold EM staining of cryosections for GNA lectin in the sporoblast. (C,D) Immuno-EM localization of γCOP in the meront (C) and sporont (D). (E,F) Immunolocalization of Sec13 in meronts (E,F, arrow) and in the sporont (F, right side). The plasmalemma of the sporont is indicated with a dashed line. (G,H) Immunolocalization of giantin-like (G, thick arrow over round profiles) and GM130-like (H, thick arrow) proteins in meronts; thin arrows in G indicate microsporidia plasma membrane. Bar, 250 nm (A); 100 nm (B-F); 180 nm (G); 120 nm (H).

the *P. grylli* spore wall, the most prevalent protein has a molecular mass of 40 kDa (p40) (Seleznev et al., 1995). Close connections of the TNs with the forming polar tube, a post-Golgi compartment, are described both elsewhere (Cali and Takvorian, 1999; Vavra and Larsson, 1999) and in the present study. This thus suggests the active participation of the TNs in polar filament formation. Thus, three *P. grylli* polar-tube proteins (PTP A, PTP B and PTP C) (Dolgikh et al., 2005) should be other examples of secretory proteins that pass through the Golgi.

To determine whether p40 and the PTP selected as cargo proteins (PTP A) (Dolgikh et al., 2005) undergo post-translational modifications in the Golgi, we examined whether these two proteins were glycosylated, because glycosylation of transported proteins is one of the main functions of the Golgi. However, this task was not trivial. All of the genes coding for the N-linked glycosylation machinery are absent in microsporidia (Katinka et al., 2001). The enzyme UDP N-acetylglucosamine: peptide N-acetylglucosaminyl transferase could participate in this process. However this enzyme carries out *O*-linked glycosylation of nuclear and cytosolic proteins in eukaryotic cells (Kreppel et al., 1997). Microsporidia also lack 'classical mammalian' *O*-linked glycosylation, where GalNAc is transferred from UDP-GalNAc onto proteins. Only three genes coding enzymes for a 'yeast' type of *O*-linked mannosylation (Lussier et al., 1997) have been found in the genome of the human microsporidia *E. cuniculi*: dolichyl-P-β-mannosyltransferase, dolichyl-P-mannose-protein *O*-mannosyltransferase and α-1,2-mannosyltransferase (Katinka et al., 2001). Of importance, the latter is considered to be Golgi specific (Lussier et al., 1997). The possibility of protein mannosylation occurring in the microsporidia Golgi is also confirmed by the presence of the Golgi GDP-mannose transporter gene in the *E. cuniculi* genome (Katinka et al., 2001).

On this basis, we first analyzed the total glycoproteins from *P. grylli* spores with periodic acid-Schiff reagent staining. The sensitivity of this method is low, and it is only reliable for highly glycosylated proteins or proteoglycans (Jay et al., 1990). This reaction did not give any decorated microsporidia bands except for the major polar tube protein of about 56 kDa (PTP A, also known as PTP-56) that was strongly labeled (Fig. 5A). Interestingly, despite the presence of a lot of membrane and secreted proteins inside cells from the insect fat body, none of them were glycosylated as strongly as PTP A. Thus, PTP A undergoes strong glycosylation.

The treatment of extracted p40 with endoglycosidase-H and *N*-glycosidase-F did not result in an electrophoresis mobility shift, in contrast to that seen with human transferrin, which was used as a positive control (not shown). This was in agreement with the absence of the N-linked glycosylation machinery in

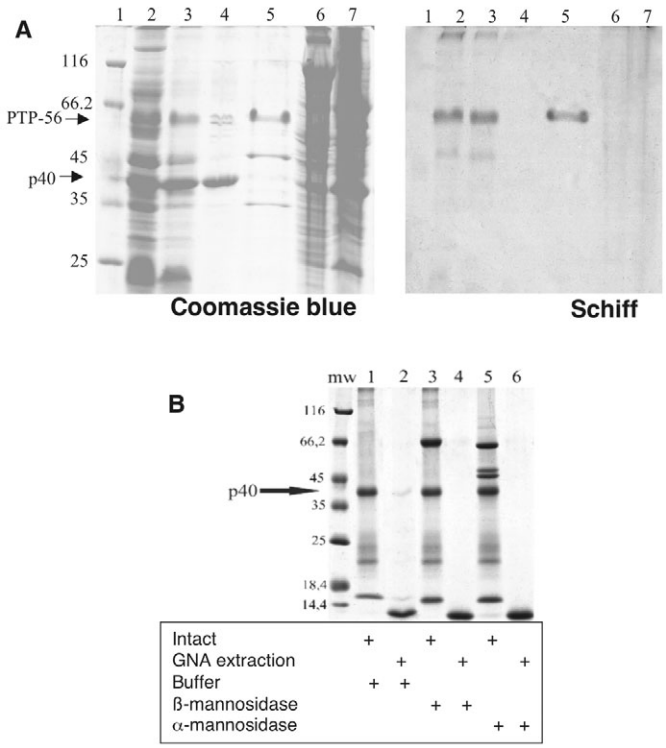

Fig. 5. Glycosylation of p40 and PTP A in microsporidia. Cells from cricket fat bodies were infected with *P. grylli* and prepared for PAGE. (A) SDS-PAGE analysis followed by Coomassie Brilliant Blue (left) and Schiff reagent (right) staining. Lane 1, MW markers; lane 2, intact spores broken up in phosphate-buffered saline and boiled for 10 minutes in SDS-PAGE sample buffer; lane 3, intact spores boiled as for lane 2; lane 4, intact *P. grylli* spores in alkaline saline solution (10 mM KOH, 170 mM KCl; 30 minutes) selectively solubilizes the major 40-kDa protein; lane 5, spore extrusion followed by washing in 3% SDS and PTPs solubilized with 50% 2-mercaptoethanol; lane 6, soluble; and lane 7, membrane, proteins of the host (cricket *Gryllus bimaculatus*) fat body. (B) Precipitation of p40 by GNA-agarose. mw, molecular weight markers; lanes 1, 3, 5, supernatant after p40 solubilization in 10 mM KOH, 170 mM KCl; lanes 2, 4, 6, proteins precipitated by GNA-agarose and eluted by boiling in SDS-PAGE sample buffer; lanes 1, 2, pretreatment with reaction buffer for mannosidase (control); lanes 3, 4, treatment with β-mannosidase; lanes 5, 6, treatment with α-mannosidase.

the genome of the human microsporidia *E. cuniculi* (Katinka et al., 2001). However, incubation of extracted p40 with *Galanthus nivalis* agglutinin (GNA; specific to the terminal α-mannose residue)-linked agarose beads showed that this protein is recognized by GNA-lectin (Fig. 5B). Moreover, this binding capacity was dramatically reduced if p40 was treated with α- or β-mannosidases. These data suggest that p40 is subjected to characteristic modifications by the microsporidia mannosyltransferases and one of them appears to be Golgi-specific (α-1, 2-mannosyltransferase of the KTR family). Altogether, these results suggest that the cargo proteins monitored undergo glycosylation in the TNs.

The major spore wall and polar tube proteins of *P. grylli* are transported through the tubular networks

If the TNs represent the Golgi, and if p40 and PTP A undergo glycosylation and apparently pass through a putative microsporidia Golgi, these proteins should undergo concentration in the TNs at defined stages in the microsporidia life cycle. To test this hypothesis, we examined the immunolocalization of p40 and the three PTPs using purified pAbs against these proteins (Dolgikh et al., 2005). In meronts, p40 was only present over the microsporidia ER cisternae (Fig. 6A,B). In sporonts, p40 concentrated over the TNs that co-localized with GM130 and giantin (our unpublished observations). In the TNs, p40 was at concentrations 3.5-fold higher than those in the ER (Table 1). At the late stages of sporogony, p40 was seen more often associated with the extended TNs (Fig. 6E,F) than with the forming spore wall, and not with the polar tube (Fig. 6D). During sporogony, the intensity of p40 labeling in the spore increased significantly, until the late stages of sporogony, with that in the *trans*-Golgi membranes being weaker than in the spore wall (Table 1).

In meronts and sporonts, the labeling of the ER and the TNs with anti-PTP Abs showed near-background levels. In sporoblasts, the process of polar filament formation was accompanied by the appearance of PTPs in the TNs. All of the anti-PTP A (Fig. 7A), anti-PTP B (not shown) and anti-PTP C (not shown) Abs demonstrated labeling of these structures. Then the labeling became visible in the initial segments of the forming polar tubes (Fig. 7A), and finally, over all of the extension of the polar filament (Fig. 7B-D). The spore walls were also labeled by anti-PTP A but not anti-PTP B and anti-PTC Abs, which could be due to the presence of similar carbohydrate antigens on the highly glycosylated molecules of PTP A and on the spore wall. Importantly, during formation of the polar tube, the labeling for the PTPs disappeared from the ER and TNs (Fig. 7B,C), although there were connections between the TNs and the polar tube (Fig. 7D). Thus, the TNs in microsporidia are the compartment through which p40, a secretory protein, and the PTPs, proteins that condense in the polar tube, pass, and where they are concentrated. These features of TNs are characteristic of Golgi.

Discussion

Previously, Golgi-like TNs in microsporidia have been considered to be clusters of vesicles (Vavra and Larsson, 1999). However, our 3D analysis has revealed that these 'vesicular Golgi zones' actually appear as networks of highly anastomosing and often varicose, tubules of 25-30 nm in diameter that are connected or associated with either the ER or the plasma membrane. Indeed, the most important finding of this study is the absence of any vesicles in these microsporidia TNs. We were not able to detect isolated vesicles using EM tomography at high 3D resolution even after quick freezing. Moreover, isolated round profiles were not seen in microsporidia even if the processes of membrane fusion and uncoating of COP-I vesicles were blocked by NEM and AlF_4 treatment, respectively. These results confirm that COP-I vesicles may not be transient.

At the same time, several lines of evidence suggest that these TNs represent the microsporidia Golgi. First, there are no other structures in microsporidia that appear suitable for the role of the Golgi. Secondly, the TNs show cytochemical characteristics of the Golgi, in that they are sensitive to osmification and to mannose-specific GNA-lectin decoration. In addition, the Golgi nature of these TNs has been confirmed

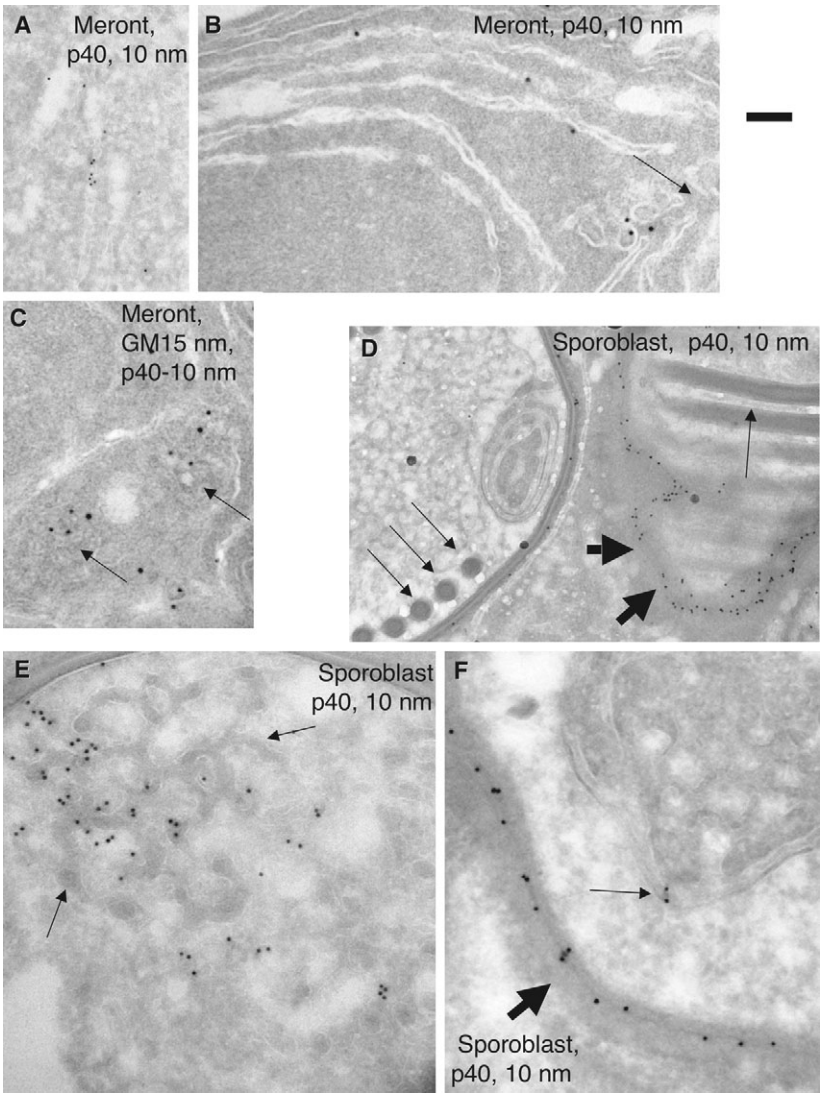

Fig. 6. Transport of p40 through the Golgi in microsporidia. Cells from cricket fat bodies were infected with *P. grylli* and prepared for cryo-immuno EM. (A-F) Cryosections of meronts (A-C) and sporoblasts (D-F) with labeling for p40. The TNs (C, thin arrows) are labeled for GM130 (15 nm; C) and p40 (10 nm; A-C). p40 can be seen over the forming spore wall (D,F, thick arrows) and in the peripheral parts of the enlarged TN (F, thin arrow), but not over the forming polar tube (E, thin arrows). Thin arrows in D indicate polar tubes. Bars, 80 nm (A-D,F); 90 nm (E).

by histochemical demonstrations of thiamine pyrophosphatase activity in the microsporidia *Glugea stephani* (Cali and Takvorian, 1999) and *P. grylli* (Sokolova et al., 2003). Finally, the TNs are the sites where the mannosylation of proteins begins.

Thus, in this study, we have demonstrated that during sporogony, microsporidia transport spore wall and polar tube components along the TNs, where these proteins undergo concentration and at least one of them is mannosylated by a Golgi-specific α-1,2-mannosyltransferase. Does this mean that ER-to-plasma membrane transport in a minimal cellular system can proceed without significant participation of COP-I- or COP-II-coated vesicles?

Microsporidia appear not to be able to promote the formation of COP-II or COP-I vesicles. According to the data from the *E. cuniculi* genome project (Katinka et al., 2001), these microsporidia have rudimentary COP-I (with six, instead of seven, subunits in their COP-I complex; ϵCOP is missing) and COP-II (the Sec24 subunit is missing) machineries. The Sec13, βCOP and β′COP-I proteins are found in *P. locustae* (see above). Using the available Abs against ϵCOP, we were not able to detect this particular COP-I subunit in *P. grylli* and *P. locustae*. Development of the *P. locustae* genome project will soon give an answer as to whether these microsporidia also have reduced COP-I and COP-II machineries. Of interest, *E. cuniculi* also lack the clathrin-based machinery that is responsible for the generation of clathrin-coated buds. The set of COP-I subunits in *E. cuniculi* (Katinka et al., 2001) appears similar to that in ldlF cells, where ϵCOP is temperature sensitive and undergoes degradation at 40°C. After degradation of the ϵ-subunit, the COP-I complex cannot form either dense coated buds or vesicles, and the uncoating of COP-I is inhibited (Guo et al., 1994). However, even at the restricted temperature, slow transportation continues in ldlF cells, as they can survive for at least two weeks under these conditions (our unpublished observations).

It is important to stress once more that the COP-I and COP-II protein machineries are present in the microsporidia genome of *E. cuniculi.* They also possess the genes encoding six of the SNAREs, four Arfs and five Rab proteins. It appears that there is a similar reduction of the main protein machines in *P. locustae* (see http://jbpc.mbl.edu/Nosema/index.html). If the coatomer is not able to form 50-60 nm vesicles, what is the function of the vesicular transport machinery in these highly simplified cells? One of the possibilities is that reduced COP complexes are used for the sorting and concentration of cargo during export from the ER, and for maturation of the tubular clusters that leads to their preparation for insertion into the plasma membrane. Their function could include, for instance, regulation of the lateral diffusion of proteins, and protein segregation along the lipid bilayer.

Since microsporidia possess several SNAREs (SNC2, synaptobrevin, syntaxin 5, VAMP, and two different copies of Bos1 and Vti1), this suggests that membrane fusion events can occur. In this case, the most plausible model of intracellular transport would be based on the formation of a cargo domain by progression mechanism in the ER (Mironov et al., 2005). This cargo domain should then somehow interact with (fuse with?) the Golgi domains. An analogous mechanism should deliver the cargo from the *trans*-Golgi compartment to the plasma membrane. The presence of two morphologically distinct domains within the TNs, one of plain tubules and the other of varicose tubules, is in line with such a proposal. During

Table 1. Quantification of the labeling densities of p40 and PTP A over different microsporidia structures in meronts and sporoblasts

	Labeling density (% ER cisternae ±s.e.)			
Protein (*n*)	ER, meront	TNs, meront	PM, sporont	PT, sporoblast
p40 (31)	100±21	298±40*	657±72*	ND
PTP A (29)	100±25	ND	432±63*	1254±67*

n, number of TN sections assessed; ND, not determined; ER, endoplasmic reticulum; TN, tubular network; PM, plasma membrane; PT, polar tube; s.e., standard error. Each value represents the mean of *n* independent measurements from at least three independent experiments (±s.e.). The data were normalized considering the mean labeling density over the ER cisternae as 100%. *Significantly different ($P \leqslant 0.05$) from labeling in the ER.

microsporidia development, the TNs are always connected/associated with the ER or the plasma membrane, indicating that this structure can serve as a shuttle that delivers cargo from the ER to the target membrane.

Could similar mechanisms of intracellular transport work in other eukaryotes? We believe that the answer is yes. First, we have data suggesting that COP-I vesicles are not the main transport carriers for either cargo proteins or Golgi enzymes (Mironov et al., 2005). Secondly, the preservation of all of the main protein machines in microsporidia suggests that the basic mechanisms of transport should be the same. If microsporidia can transport cargo without the use of COP-I and COP-II vesicles, this means that this possibility should be tested for in mammalian cells. Our analysis shows that there are no strong results that consistently demonstrate that COP-I and COP-II vesicles are transport carriers (see Mironov et al., 2003; Mironov et al., 2005; Kweon et al., 2004). At this stage, it is preliminary to state that COP-I and COP-II vesicles are not important for intracellular transport. However, one possibility is that they serve different roles (i.e. not as the main transport containers). We now have data that support at least two additional functions for COP-I vesicles: one is their role in the regulation of the Golgi shape (COPI vesicles control Golgi morphology by acting as a reservoir for membrane curvature) (G.V.B., unpublished results) and the other is their role in the regulation of fusion between Golgi cisternae by the extraction of membrin and GOS28 from cisternae by COP-I vesicles (Volchuk et al., 2004; Cosson et al., 2005) (M.M., unpublished results). Another interesting point is the rarity of COP-I-dependent vesicles in the Golgi of the yeast *Saccharomyces cerevisiae* (Kepes et al., 2005). Therefore, we believe that this model is not unique to the microsporidian group.

Materials and Methods

Antibodies

The following antibodies (Abs) were used: polyclonal Ab (pAb) against human GM130 and giantin (Marra et al., 2001); pAb against γ-subunit of plant (*Arabidopsis thaliana*) COP-I (Pimpl et al., 2000); pAbs against different subunits of mammalian, yeast and plant COP-I from: F. Wieland, Heidelberg University, Germany (Faulstich et al., 1996); D. Robinson, Heidelberg University, Germany (Pimpl et al., 2000); M. Krieger, Massachusetts Institute of Technology, Cambridge, MA (Guo et al., 1994); R. Duden, University of Cambridge, Cambridge, UK (Eugster et al., 2004); S. Coughlan, Agilent Technologies, Wilmington, DE (Pimpl et al., 2000). Abs against *P. grylli* structural proteins of spore wall and polar tube (p40 and PTP A, see below) were generated and purified as described previously (Dolgikh et al., 2005).

To prepare pAbs against the microsporidian homolog of Sec13, primers were designed according to the coding sequence from the *Nosema locustae* Genome Project (http://jbpc.mbl.edu/Nosema/ index.html, *Nosema locustae* Genome Project, Marine Biological Laboratory at Woods Hole): 5′-ggatccGATGGAGGTGCA-GAGGGAGATCATACAC-3′ (direct); 5′-gaattcTTATTCAGACTTCTTCAGCGG-3′ (reverse). The encoding gene was amplified by PCR with *Pfu* polymerase and *P. locustae* genomic DNA as a template, cloned into pBlueScript KS(+) (Stratagene) and finally inserted into the prokaryotic expression vector pRSETb (Invitrogen, CA) using *Bam*HI and *Eco*RI sites. Expression was carried out in the C41 derivative of the *Escherichia coli* BL21(DE3) strain (Miroux and Walker, 1996).

Bacteria were sonicated in 50 mM sodium phosphate, pH 7.5, 0.3 M NaCl and the inclusion bodies containing recombinant protein were isolated by centrifugation at 1500 ***g*** for 10 minutes. The pellets were carefully washed with the same solution containing 0.05% Triton X-100 and the inclusion bodies were solubilized in 8 M urea. The solubilized protein was diluted tenfold with 50 mM sodium phosphate, 0.3 M NaCl, mixed with an equal volume of Freund's Adjuvant Complete (Sigma) and used for immunization. Rabbits were immunized by three intramuscular injections (about 0.3 mg protein per injection) at 10-day intervals. Ten days after the last immunization, 15 ml of blood was collected. The serum was analyzed by immunoblotting with proteins from the various intracellular stages of *P. locustae*. These proteins are also under further analysis (V.V.D., unpublished results).

Nanogold-conjugated Fab fragments of anti-rabbit IgG and Gold Enhancer were from Nanoprobes (USA). Protein A conjugated with colloidal gold was from J. Slot

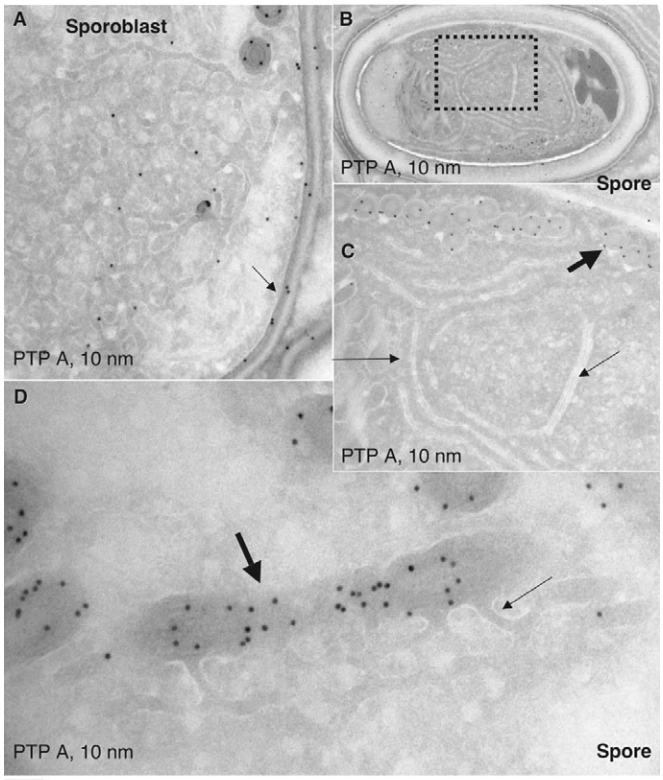

Fig. 7. Transport of PTP A through the Golgi in microsporidia. Cells from cricket fat bodies were infected with *P. grylli* and prepared for cryo-immuno EM. Cryosections of a sporoblast (A) and maturing spores (B-D) with labeling for PTP A. (C) represents the enlarged area from the black box in B. (A) PTP A is concentrated over the large TN (thin arrow, forming spore). (B-D), PTP A is visible over polar tubes (thick arrows), but not over the ER (C, thin arrows). Polar tubes are connected with the TN (D, thin arrow). Bars, 100 nm (A,C); 300 nm (B); 70 nm (D).

(Utrecht University, Utrecht, The Netherlands). Anti-rabbit, anti-mouse and anti-sheep Abs conjugated with Alexa Fluor 488, Alexa Fluor 546 and Alexa Fluor 633 were from Molecular Probes Europe BV (The Netherlands). Unless otherwise stated, all other chemicals and reagents were obtained from previously described sources (Trucco et al., 2004).

Treatment of samples

To block SNARE-dependent membrane fusion, samples from the insect fat bodies were treated for 10 minutes at 4°C with 1 M NEM dissolved in PBS, and then for 2 minutes with DTT, washed with medium, then re-warmed to 37°C, fixed 10 minutes after re-warming, and prepared for EM and EM tomography (Mironov et al., 2001; Mironov et al., 2003). To inhibit the uncoating of COP-I, samples from the insect fat body were treated with AlF_4 (20 mM NaF; 50 μM $AlCl_3$) in medium for 20 minutes (Cole et al., 1996), and then prepared for EM and EM tomography.

Analysis of protein glycosylation

To assess protein glycosylation, glycoprotein-specific periodic-acid-Schiff reagent staining was performed, according to the standard protocol. Briefly, after sodium dodecyl sulfate (SDS)-PAGE, the gels were fixed overnight in 40% ethanol, 5% acetic acid at room temperature, and then sequentially incubated in 0.7% periodic acid, 5% acetic acid for 2 hours, 0.2% sodium metabisulfite, 5% acetic acid for 2 hours and Schiff reagent overnight. To prepare the Schiff reagent, 1.0 g fuchsine basic (rosaniline) was dissolved in 100 ml water and 20 ml 1.0 N HCl, and 1.7 g sodium metabisulfite was added. After stirring for 15 minutes, the mixture was cleared by incubation with activated charcoal. The carbon precipitate was removed by centrifugation (Gallagher, 1998).

For N-glycosidase-F treatment of p40, intact spores were incubated at 100°C for 10 minutes in 0.1 M Tris-HCl, pH 8.0, 2% SDS, 5% 2-mercaptoethanol. The spores were precipitated, and the supernatant was diluted tenfold, with additions for the final concentrations of 0.1 M Tris-HCl, pH 8.0, 0.2% SDS, 0.5% 2-mercaptoethanol, 10 mM EDTA, 1% Triton X-100, and 5 U/ml N-glycosidase-F. The reaction was left overnight at 4°C and reaction mixture was analysed by SDS-PAGE. Human transferrin was incubated under the same conditions as a positive control. To recognize α-mannose and β-mannose, p40 was selectively extracted from intact spores by their incubation in alkaline-saline solution (10 mM KOH, 170 mM KCl) (Dolgikh et al., 2005), and neutralization with 0.05 volumes of 1.0 M sodium phosphate (pH 6.0) was followed by the incubation either overnight at room temperature or at 37°C for 3 hours in the presence 0.1 U α-mannosidase or β-mannosidase. The control and enzyme-treated samples were incubated for 1 hour at room temperature in the presence of GNA-lectin crosslinked with agarose beads. The agarose was pre-equilibrated with 50 mM Na-phosphate buffer, pH 6.0, 170 mM NaCl. The beads were carefully washed in the same buffer following this incubation. The washed and precipitated proteins were eluted by boiling the agarose with 50 μl sample buffer for 10 minutes, and analyzed by SDS-PAGE. The volumes of the media for protein precipitation with agarose (neutralized protein extract) and sample buffer for the elution were equal.

Immunoblotting, immunofluorescence analysis and immunoelectron microscopy

P. grylli and *P. locustae* spores and their intracellular stages were purified from the fat bodies of infected *Gryllus bimaculatus* crickets by Percoll density gradient centrifugation, as described previously (Seleznev et al., 1995). Spores were disrupted by vortexing with glass beads (Bio-Rad, Milan, Italy) in phosphate-buffered saline, for 30 minutes at 4°C. The samples for SDS-PAGE were boiled with an equal volume of 2× sample buffer (125 mM Tris-HCl pH 6.8, 4% SDS, 10% 2-mercaptoethanol, 20% glycerol) and the proteins were separated by SDS-PAGE (Laemmli, 1970) before being transferred to nitrocellulose membranes by the standard semi-dry method, according to the instructions for the electroblotting apparatus. The membranes were incubated for 1 hour in TTBS (50 mM Tris-HCl pH 7.4, 150 mM NaCl, 0.05% Tween-20) with 1% BSA (blocking solution), washed with TTBS and incubated overnight at 4°C with the first Abs. The purified Abs against *P. grylli* structural proteins of the spore wall and polar tube (p40 and PTP A) were used undiluted. The anti-giantin and anti-GM130 Abs were diluted 1:2000. The serum against the *P. locustae* homolog of Sec13 was diluted 1:500. After a careful wash with TTBS, the membranes were incubated for 1 hour with anti-rabbit IgG conjugated with peroxidase (Sigma, Milan, Italy) that was diluted 1:3000 in blocking solution, and washed again with TTBS. The peroxidase reaction was then performed with 4-chloro-1-naphthol as substrate.

For immunofluorescence, the fat bodies of infected crickets were homogenized in phosphate-buffered saline, placed on poly-lysine-treated glass cover slips, incubated for 5 minutes, fixed with 4% paraformaldehyde for 15 minutes, washed with phosphate-buffered saline and coated with 5% gelatin. The cells were permeabilized by incubation in blocking solution (phosphate-buffered saline, 0.05% saponin, 0.1% Triton X-100, 50 mM NaCl, 0.5% BSA) for 1 hour, and then incubated with a 1:1000 dilution of the anti-giantin Ab. They were finally washed in phosphate-buffered saline and prepared for immunofluorescence, as previously described (Mironov et al., 2001).

Electron microscopy

For EM, fragments of the fat bodies of *P. grylli* infected and *P. locustae* infected crickets were fixed in 1% glutaraldehyde as previously described (Mironov et al., 2001). Conventional EM, fast-freezing and low-temperature embedding into an acrylic resin (LR White) (Sokolova et al., 2001), 3D reconstructions of EM serial sections, ultrathin cryosectioning and analysis of samples by EM tomography were all carried out as previously described (Mironov et al., 2001; Kweon et al., 2004).

For visualization of the *cis*-Golgi, the samples were directly stained with 1% OsO_4 for 24-72 hours, as previously described (Novikoff and Goldfischer, 1961). In some cases samples were prefixed with 0.05% glutaraldehyde for 20 minutes. For cryosection immuno-gold EM, the purified p40 and PTP A pAbs were concentrated ~20-fold in centrifuge concentrators (Sartorius, Germany) and then diluted in blocking solution. Cryosections and sections from LR White blocks were incubated with anti-giantin (1:100), anti-GM130 (1:50), anti-γ-COP (1:100), anti-microsporidian Sec13 homolog (1:300), anti-p40 (undiluted), anti-PTP A (undiluted) pAbs or with GNA conjugated with nano-gold (1:20) for 2 hours. To enhance the availability of the IgG fractions specific for microsporidia proteins, we used a high (1%) concentration of acetylated bovine serum albumin (BSA-c from AURION, Wageningen, The Netherlands) to block the background. The microsporidia stages were classified according to Vavra and Larsson (Vavra and Larsson, 1999).

We thank C. P. Berrie for critical reading of the manuscript, A. A. Mironov, Jr and R. S. Polishchuk for helpful discussions. F. Wieland, D. Robinson, M. Krieger, S. Coughlan, R. Duden for providing antibodies. We acknowledge financial support from INTAS (Project 99-4-1732), an INTAS Fellowship for Young Scientists (YSF 2001/2-0064 to V.V.D.), the Russian Foundation of Basic Research (grant no. 05-04-49616) and the Italian National Research Council (contract no. 01.00035.PF49).

References

Bannykh, S. I., Rowe, T. and Balch, W. E. (1996). The organization of endoplasmic reticulum export complexes. *J. Cell Biol.* **135**, 19-35.

Beznoussenko, G. V. and Mironov, A. A. (2002). Models of intracellular transport and evolution of the Golgi complex. *Anat. Rec.* **268**, 226-238.

Bohne, W., Ferguson, D. J., Kohler, K. and Gross, U. (2000). Developmental expression of a tandemly repeated, glycine- and serine-rich spore wall protein in the microsporidian pathogen Encephalitozoon cuniculi. *Infect. Immunol.* **68**, 2268-2275.

Bonfanti, L., Mironov, A., Jr, Martinez-Menarguez, J., Martella, O., Fusella, A., Baldassare, M., Buccione, R., Geuze, H., Mironov, A. and Luini, A. (1998). Procollagen traverses the Golgi stack without leaving the lumen of cisternae: evidence for cisternal maturation. *Cell* **95**, 993-1003.

Cali, A. and Takvorian, P. M. (1999). Developmental morphology and life cycles of the microsporidia. In *The Microsporidia and Microsporidiosis* (ed. M. Wittner and L. M. Weiss), pp. 85-128. Washington, DC: American Society for Microbiology.

Cole, N. B., Sciaky, N., Marotta, A., Song, J. and Lippincott-Schwartz, J. (1996). Golgi dispersal during microtubule disruption: regeneration of Golgi stacks at peripheral endoplasmic reticulum exit sites. *Mol. Biol. Cell* **7**, 631-650.

Cosson, P., Ravazzola, M., Varlamov, O., Sollner, T. H., Di Liberto, M., Volchuk, A., Rothman, J. E. and Orci, L. (2005). Dynamic transport of SNARE proteins in the Golgi apparatus. *Proc. Natl. Acad. Sci. USA* **102**, 14647-14652.

Delbac, F., Peyret, P., Metenier, G., David, D., Danchin, A. and Vivares, C. P. (1998). On proteins of the microsporidian invasive apparatus: complete sequence of a polar tube protein of Encephalitozoon cuniculi. *Mol. Microbiol.* **29**, 825-834.

Dolgikh, V. V., Semenov, P. B., Mironov, A. A. and Beznoussenko, G. V. (2005). Immunocytochemical identification of the major exospore protein and three polar-tube proteins of the microsporidia *Paranosema grylli*. *Protist* **156**, 77-87.

Eugster, A., Frigerio, G., Dale, M. and Duden, R. (2004). The alpha- and beta'-COP WD40 domains mediate cargo-selective interactions with distinct di-lysine motifs. *Mol. Biol. Cell* **15**, 1011-1123.

Faulstich, D., Auerbach, S., Orci, L., Ravazzola, M., Wegchingel, S., Lottspeich, F., Stenbeck, G., Harter, C., Wieland, F. T. and Tschochner, H. (1996). Architecture of coatomer: molecular characterization of delta-COP and protein interactions within the complex. *J. Cell Biol.* **135**, 53-61.

Gallagher, S. R. (1998). One-dimensional SDS gel electrophoresis of proteins. In *Current Protocols in Cell Biology*, pp. 6.1.1.-6.1.34. New York: John Wiley.

Griffiths, G., Fuller, S. D., Back, R., Hollinshead, M., Pfeiffer, S. and Simons, K. (1989). The dynamic nature of the Golgi complex. *J. Cell Biol.* **108**, 277-297.

Guo, Q., Vasile, E. and Krieger, M. (1994). Disruptions in Golgi structure and membrane traffic in a conditional lethal mammalian cell mutant are corrected by epsilon-COP. *J. Cell Biol.* **125**, 1213-1224.

Hayman, J. R., Hayes, S. F., Amon, J. and Nash, T. E. (2001). Developmental expression of two spore wall proteins during maturation of the microsporidian Encephalitozoon intestinalis. *Infect. Immun.* **69**, 7057-7066.

Hirschberg, K., Miller, C. M., Ellenberg, J., Presley, J. F., Siggia, E. D., Phair, R. D. and Lippincott-Schwartz, J. (1998). Kinetic analysis of secretory protein traffic and characterization of golgi to plasma membrane transport intermediates in living cells. *J. Cell Biol.* **143**, 1485-1503.

Jay, G. D., Culp, D. J. and Jahnke, M. R. (1990). Silver staining of extensively glycosylated proteins on sodium dodecyl sulfate-polyacrylamide gels:enhancement by carbohydrate-binding dyes. *Anal. Biochem.* **185**, 324-330.

Katinka, M. D., Duprat, S., Cornillot, E., Metenier, G., Thomarat, F., Prensier, G., Barbe, V., Peyretaillade, E., Brottier, P., Wincker, P. et al. (2001). Genome sequence and gene compaction of the eukaryote parasite Encephalitozoon cuniculi. *Nature* **414**, 450-453.

Keohane, E. M. and Weiss, L. M. (1999). The structure, function, and composition of the microsporidian polar tube. In *The Microsporidia and Microsporidiosis* (ed. M. Wittner and L. M. Weiss), pp. 196-224. Washington, DC: American Society for Microbiology.

Kepes, F., Rambourg, A. and Satiat-Jeunemaitre, B. (2005). Morphodynamics of the secretory pathway. *Int. Rev. Cytol.* **242**, 55-120.

Kreppel, L. K., Blomberg, M. A. and Hart, G. W. (1997). Dynamic glycosylation of nuclear and cytosolic proteins. *J. Biol. Chem.* **272**, 9308-9315.

Kweon, H.-S., Beznoussenko, G. V., Micaroni, M., Polishchuk, R. S., Trucco, A., Martella, O., Di Giandomenico, D., Marra, P., Fusella, A., Di Pentima, A. et al. (2004). Golgi enzymes are enriched in perforated zones of Golgi cisternae but are depleted in COP-I vesicles. *Mol. Biol. Cell* **15**, 4710-4724.

Ladinsky, M. S., Mastronarde, D. N., McIntosh, J. R., Howell, K. E. and Staehelin, L. A. (1999). Golgi structure in three dimensions: functional insights from the normal rat kidney cell. *J. Cell Biol.* **144**, 1135-1149.

Ladinsky, M. S., Wu, C. C., McIntosh, S., McIntosh, J. R. and Howell, K. E. (2002). Structure of the Golgi and distribution of reporter molecules at 20 degrees C reveals the complexity of the exit compartments. *Mol. Biol. Cell* **13**, 2810-2825.

Laemmli, U. K. (1970). Cleavage of structural proteins during the assembly of the head of bacterophage T4. *Nature* **277**, 680-685.

Lussier, M., Sdicu, A. M., Bussereau, F., Jacquet, M. and Bussey, H. (1997). The Ktr1p, Ktr3p, and Kre2p/Mnt1p mannosyltransferases participate in the elaboration of yeast O- and N-linked carbohydrate chains. *J. Biol. Chem.* **272**, 15527-15531.

Marra, P., Maffucci, T., Daniele, T., Tullio, G. D., Ikehara. Y., Chan, E. K., Luini, A., Beznoussenko, G., Mironov, A. and De Matteis, M. A. (2001). The GM130 and GRASP65 Golgi proteins cycle through and define a subdomain of the intermediate compartment. *Nat. Cell Biol.* **3**, 1101-1113.

McIntosh, J. R. (2001). Electron microscopy of cells: a new beginning for a new century. *J. Cell Biol.* **153**, F25-F32.

Mironov, A. A., Beznoussenko, G. V., Nicoziani, P., Martella, O., Trucco, A., Kweon, H.-S., Di Giandomenico, D., Polishchuk, R. S., Fusella, A., Lupetti, P. et al. (2001). Small cargo proteins and large aggregates can traverse the Golgi by a common mechanism without leaving the lumen of cisternae. *J. Cell Biol.* **155**, 1225-1238.

Mironov, A. A., Mironov, A. A., Jr, Beznoussenko, G. V., Trucco, A., Lupetti, P., Smith, J. D., Geerts, W. J., Koster A. J., Burger K. N., Martone M. E. et al. (2003). ER-to-Golgi carriers arise through direct en bloc protrusion and multistage maturation of specialized ER exit domains. *Dev. Cell* **5**, 583-594.

Mironov, A. A., Beznoussenko, G. V., Polishchuk, R. S. and Trucco, A. (2005). Intra-Golgi transport: a way to a new paradigm? *Biochim. Biophys. Acta* **1744**, 340-350.

Miroux, B. and Walker, J. E. (1996). Over-production of proteins in Escherichia coli: mutant hosts that allow synthesis of some membrane proteins and globular proteins at high levels. *J. Mol. Biol.* **260**, 289-298.

Novikoff, A. B. and Goldfischer, S. (1961). Nucleoside-diphosphatase activity in the Golgi apparatus and its usefulness for cytological studies. *Proc. Natl. Acad. Sci. USA* **47**, 802-810.

Opat, A. S., van Vliet, C. and Gleeson, P. A. (2001). Trafficking and localisation of resident Golgi glycosylation enzymes. *Biochimie* **83**, 763-773.

Orci, L., Glick, B. S. and Rothman, J. E. (1986). A new type of coated vesicular carrier that appears not to contain clathrin: its possible role in protein transport within the Golgi stack. *Cell* **46**, 171-184.

Pimpl, P., Movafeghi, A., Coughlan, S., Denecke, J., Hillmer, S. and Robinson, D. G. (2000). In situ localization and in vitro induction of plant COP-I-coated vesicles. *Plant Cell* **12**, 2219-2236.

Rabouille, C., Hui, N., Hunte, F., Kieckbusch, R., Berger, E. G., Warren, G. and Nilsson, T. (1995). Mapping the distribution of Golgi enzymes involved in the construction of complex oligosaccharides. *J. Cell Sci.* **108**, 1617-1627.

Scales, S. J., Pepperkok, R. and Kreis, T. E. (1997). Visualization of ER-to-Golgi transport in living cells reveals a sequential mode of action for COP-II and COP-I. *Cell* **90**, 1137-1148.

Seleznev, K., Issi, I., Dolgikh, V., Belostotskaya, G., Antonova, O. and Sokolova, J. (1995). Fractionation of different life cycle stages of microsporidia Paranosema grylli from crickets Gryllus bimaculatus by centrifugation in percoll density gradient for biochemical research. *J. Eukaryot. Microbiol.* **42**, 288-292.

Sokolova, Y., Snigirevskaya, E. S., Skarlato, S. O., Komissarchik, Y. Y. and Mironov, A. A. (2001). Unusual Golgi apparatus at the proliferative stage of microsporidian life cycle. *Dokl. Biol. Sci.* **378**, 290-293.

Sokolova, Y. Y., Dolgikh, V. V., Morzhina, E. V., Nassonova, E. S., Issi, I. V., Terry, R. S., Ironside, J. E., Smith, J. E. and Vossbrinck, C. R. (2003). Establishment of the new genus Paranosema based on the ultrastructure and molecular phylogeny of the type species Paranosema grylli Gen. Nov., Comb. Nov. (Sokolova, Selezniov, Dolgikh, Issi 1994), from the cricket Gryllus bimaculatus Deg. *J. Invertebr. Pathol.* **84**, 159-172.

Sokolova, Y. Y., Issi, I. V., Morzhina, E. V., Tokarev, Y. S. and Vossbrinck, C. R. (2005). Ultrastructural analysis supports transferring Nosema whitei Weiser 1953 to the genus Paranosema and creation a new combination, Paranosema whitei. *J. Invertebr. Pathol.* **90**, 122-126.

Trucco, A., Polishchuk, R. S., Martella, O., Di Pentima, A., Fusella, A., Di Giandomenico, D., San Pietro, E., Beznoussenko, G. V., Polishchuk, E. V., Baldassarre, M. et al. (2004). Secretory traffic triggers the formation of tubular continuities across Golgi sub-compartments. *Nat. Cell Biol.* **6**, 1071-1081.

Vavra, J. and Larsson, J. I. R. (1999). Structure of the microsporidia. In *Microsporidia and Microsporidiosis* (ed. M. Wittner and L. M. Weiss), pp. 7-84. Washington, DC: American Society for Microbiology.

Volchuk, A., Ravazzola, M., Perrelet, A., Eng, W. S., Di Liberto, M., Varlamov, O., Fukasawa, M., Engel, T., Sollner, T. H., Rothman, J. E. et al. (2004). Countercurrent distribution of two distinct SNARE complexes mediating transport within the Golgi stack. *Mol. Biol. Cell* **15**, 1506-1518.